

at initiating disease, which could be determined by injecting mPFFs produced under varying conditions or even injecting lysate from PD cases. With further characterization, this model will doubtlessly be of use in elucidating the pathogenesis of PD and in developing therapeutic strategies that may prove efficacious in patients following testing in this model.

#### REFERENCES

- Braak, H., Del Tredici, K., Rüb, U., de Vos, R.A.I., Jansen Steur, E.N.H., and Braak, E. (2003). Staging of brain pathology related to sporadic Parkinson's disease. *Neurobiol. Aging* *24*, 197–211.
- Brundin, P., and Melki, R. (2017). Prying into the prion hypothesis for Parkinson's disease. *J. Neurosci.* *37*, 9808–9818.
- Kalia, L.V., and Lang, A.E. (2015). Parkinson's disease. *Lancet* *386*, 896–912.
- Killinger, B.A., Madaj, Z., Sikora, J.W., Rey, N., Haas, A.J., Vepa, Y., Lindqvist, D., Chen, H., Thomas, P.M., Brundin, P., et al. (2018). The vermiform appendix impacts the risk of developing Parkinson's disease. *Sci. Transl. Med.* *10*, eaar5280.
- Kim, S., Kwon, S.-H., Kam, T.-I., Panicker, N., Karuppagounder, S.S., Lee, S., Lee, J.H., Kim, W.R., Kook, M., Foss, C.A., et al. (2019). Transneuronal propagation of pathologic  $\alpha$ -synuclein from the gut to the brain models Parkinson's disease. *Neuron* *103*, this issue, 627–641.
- Klingenhoefer, L., and Reichmann, H. (2015). Pathogenesis of Parkinson disease—the gut-brain axis and environmental factors. *Nat. Rev. Neurol.* *11*, 625–636.
- Sacino, A.N., Brooks, M., Thomas, M.A., McKinney, A.B., Lee, S., Regenhardt, R.W., McGarvey, N.H., Ayers, J.I., Notterpek, L., Borchelt, D.R., et al. (2014). Intramuscular injection of  $\alpha$ -synuclein induces CNS  $\alpha$ -synuclein pathology and a rapid-onset motor phenotype in transgenic mice. *Proc. Natl. Acad. Sci. USA* *111*, 10732–10737.
- Sulzer, D., and Surmeier, D.J. (2013). Neuronal vulnerability, pathogenesis, and Parkinson's disease. *Mov. Disord.* *28*, 715–724.

## Ganglion Cells in Primate Retina Use Fuzzy Logic to Encode Complex Visual Receptive Fields

Jeffrey S. Diamond<sup>1,\*</sup>

<sup>1</sup>Synaptic Physiology Section, NINDS Intramural Research Program, National Institutes of Health, Bethesda, MD 20892, USA

\*Correspondence: [diamondj@ninds.nih.gov](mailto:diamondj@ninds.nih.gov)

<https://doi.org/10.1016/j.neuron.2019.08.003>

In most neurons, all spikes look alike. However, in this issue of *Neuron*, Rhoades et al. (2019) describe a ganglion cell in primate retina that reports visual input to different regions of its receptive field with distinct action potential waveforms.

The visual world enters our nervous system via an array of more than 120 million photoreceptors in each retina and encounters roughly the same number of neurons in the primary visual cortex (Leuba and Kraftsik, 1994). In between, about 20 distinct representations of the visual world are formed by the retinal circuitry and then transmitted through the optic nerve by just 1 million retinal ganglion cell (RGC) axons. It stands to reason then that each action potential passing through this “bottleneck” (Van Essen et al., 1992) ought to encode as much information as possible. One might therefore expect individual RGCs to exhibit complex spiking behavior and intricate receptive field (RF) characteristics. In monkey retina, however, most ganglion cells exhibit relatively simple RFs (Gauthier et al., 2009), perhaps suggesting that, at least in primates, most sophisticated vi-

sual processing is performed by more elaborate cortical circuits.

Most of what we understand about primate RGCs, however, comes from studies of a few subtypes that make up the majority of the overall population (Dacey, 1999): midget (ON and OFF), parasols (ON and OFF), and small bistratified (ON-OFF). These RGC subtypes exhibit relatively simple center-surround receptive fields that are traditionally represented by two-dimensional Gaussian functions, although they do exhibit minor irregularities that enable each subtype to sample visual space completely (Figures 1A and 1B; Gauthier et al., 2009). More complex RF properties, such as sensitivity to looming shapes or directional motion observed in RGCs of lower mammals, have been harder to come by in the primate (although see Manookin et al., 2018). Without many of the genetic tools

available in mouse, it is difficult to identify consistently and record from less common RGC subtypes.

In this issue of *Neuron*, Rhoades et al. (2019) overcome these limitations by recording visual responses from hundreds of RGCs simultaneously in monkey retina mounted on a multielectrode array (MEA). Many of the 519 densely arranged extracellular electrodes record action potentials from several cells and, in turn, each RGC's activity typically is picked up by multiple electrodes, enabling responses to be recorded from the large majority of the RGCs on the array. After responses to spatiotemporally noisy visual stimuli are collected, spikes are assigned (“sorted”) to individual cells according to spike shape and the “electrical image” of electrodes across the array that detect simultaneously signals arising from each single RGC. Spatiotemporal RF properties are



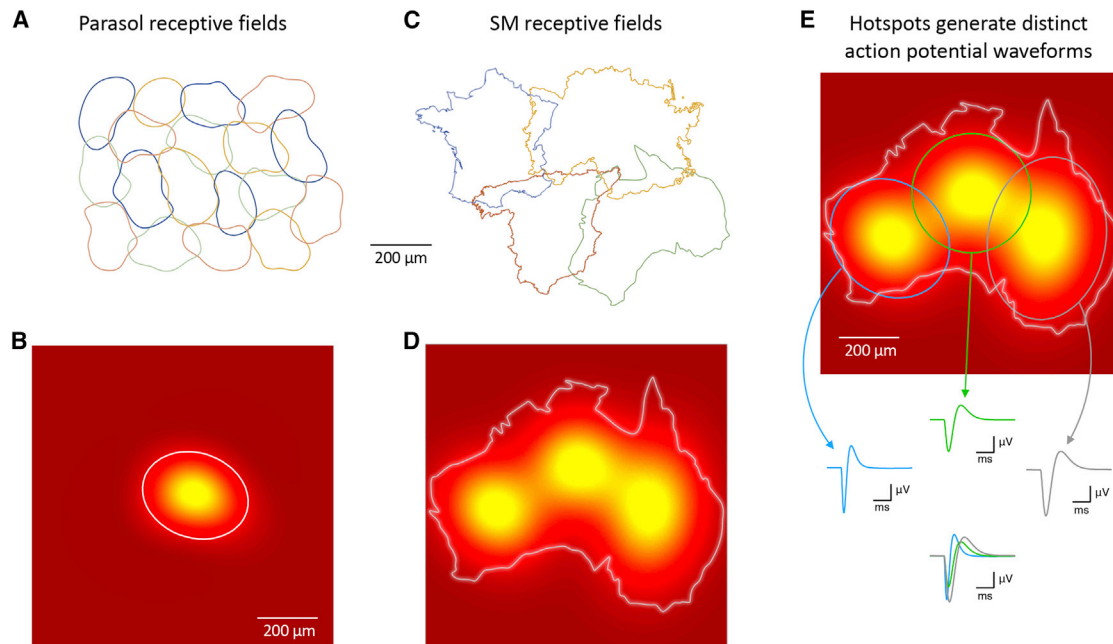


**Figure 1. Smooth Monostratified Ganglion Cells Exhibit Complex Receptive Fields and Diverse Spike Waveforms**

(A) Schematic showing a mosaic tiling of relatively simple parasol ganglion cell receptive fields. (B) The receptive field of a single parasol cell is typically well fit by a two-dimensional Gaussian function. The contour indicates the level that is 20% of the maximum. (C) Smooth monostratified cells exhibit highly irregular receptive field shapes. (D) The receptive field of an individual smooth monostratified cell comprises computationally distinct “hotspots.” (E) Activation of different hotspots give rise to distinct action potential signatures in extracellular recordings.

determined by averaging the 200-ms clips of the stimulus movie preceding each spike (Chichilnisky, 2001); cells within a subtype are grouped together according to similar RF characteristics (in space, time, and color), and the categorization is verified by checking that the spatial RFs within a subtype form a tiled mosaic across the retina (Figure 1A). With this approach, it is possible to classify even relatively sparse subtypes and measure their RFs with very high spatial resolution (Field et al., 2010).

Here, Rhoades et al. (2019) focus on ON and OFF smooth monostratified (SM) RGCs, which previously had been studied only one at a time with intracellular recordings (Crook et al., 2008). Their MEA recordings reveal that, in contrast to midget and parasol RGCs, SM cells exhibit highly irregular RFs marked by multiple spatially separated hotspots (e.g., Figures 1C and 1D). Further analysis confirms that these hotspots do not reflect inputs from multiple, mischaracterized cells but are, in fact, part of a single RGC’s receptive field. The hotspots are larger than expected if they were due to input from individual presynaptic bipolar cells, the usual source of RF subunits, and they exhibit nonlinear

response properties, suggesting that complex presynaptic circuitry drives responses within each hotspot.

By itself, evidence that a primate RGC exhibits spatially distinct, nonlinear subunits within its RF is enough to suggest that visual processing in the primate retina may be more complex than previously thought (see also Crook et al., 2008). But wait, there’s more: after determining the RF of SM cells with full-field stimulation, Rhoades et al. (2019) stimulate hotspots individually or together and find that they combine nonlinearly to drive the cell’s spike response. This result begs all sorts of questions about the nature of hotspot interactions and their consequent visual computations, most of which would be difficult to answer without knowing which hotspot contributes most to a particular response.

During the course of this study, however, the SM cell reveals another remarkable property that hints at even greater complexity and, at the same time, presents a key to unraveling its complicated physiology: each hotspot elicits its own distinct action potential waveform on the electrode array, including those electrodes located beneath the soma (Figure 1E). This surpris-

ing finding suggests that spikes originate in different dendritic regions and thereby report activation of each hotspot to the cell body with a distinctive signature, a kind of “fuzzy logic” that could enrich the information in the cell’s spike response beyond that transmitted in a binary signal (Zadeh, 1965). It also provides interesting insights into how the cell integrates inputs from different hotspots. Full-field noise stimulation elicits action potentials that can be clustered into different groups corresponding to individual RF hotspots, with no apparent intermediate waveforms that might reflect combined contributions from multiple hotspots. This suggests that individual hotspots might acquire veto power over others by virtue of the strength or timing of their activation. Consistent with this idea, spike inputs from different hotspots reach the soma with delays that can differ between hotspots by as much as 0.5 ms, yet somatic spiking observes a 1.7 ms refractory period, suggesting that the hotspot activated earliest may take precedence.

The results presented here raise interesting questions about visual processing in SM cells and also may cast doubt

on long-held assumptions about neural signaling. First, what aspects of the visual world do SM cells actually compute? Rhoades et al. (2019) present simulations suggesting that hotspots represent distinct computational units and that complicated models will be required to capture the full extent of the cell's behavior, but the specific visual features that are encoded by SM cells remain to be determined.

A second question concerns how the hotspot-specific spike signatures influence the signals communicated by SM cells to higher visual centers. One would expect that the powerful active conductances in the cell's axon hillock would transform each of these distinct signals into a common, stereotyped waveform that propagates down the axon through the optic nerve. In this case, RF-specific information might be lost in transmission to downstream targets in the lateral geniculate nucleus, superior colliculus or other visual areas. Although not addressed explicitly here by Rhoades et al. (2019), some of the data suggest that SM cells may surprise us once again. In many cases, the electrical image of an RGC recorded on MEA includes signals in the axon as action potentials propagate from the RGC soma along the inner surface of the retina to the

optic disk, where they enter the optic nerve. If axonal action potentials exhibited the same shape regardless of originating hotspot, one would expect that  $n$  hotspots would give rise to  $n+1$  clusters of action potential waveforms, the extra group comprising propagating impulses in the axon. In an illustrated example in which the electrical image includes the axon (e.g., Figure 5B in Rhoades et al., 2019), however, this appears not to be the case: three hotspots produce three clusters, not four, suggesting that propagating action potentials may preserve the signaling diversity generated by the hotspots. Future experiments may reveal the visual features computed via this unorthodox RF organization and determine whether SM axons really do communicate their fuzzy logic to higher visual centers.

#### REFERENCES

- Chichilnisky, E.J. (2001). A simple white noise analysis of neuronal light responses. *Network* 12, 199–213.
- Crook, J.D., Peterson, B.B., Packer, O.S., Robinson, F.R., Gamlin, P.D., Troy, J.B., and Dacey, D.M. (2008). The smooth monostriated ganglion cell: evidence for spatial diversity in the Y-cell pathway to the lateral geniculate nucleus and superior colliculus in the macaque monkey. *J. Neurosci.* 28, 12654–12671.
- Dacey, D.M. (1999). Primate retina: cell types, circuits and color opponency. *Prog. Retin. Eye Res.* 18, 737–763.
- Field, G.D., Gauthier, J.L., Sher, A., Greschner, M., Machado, T.A., Jepsen, L.H., Shlens, J., Gunning, D.E., Mathieson, K., Dabrowski, W., et al. (2010). Functional connectivity in the retina at the resolution of photoreceptors. *Nature* 467, 673–677.
- Gauthier, J.L., Field, G.D., Sher, A., Greschner, M., Shlens, J., Litke, A.M., and Chichilnisky, E.J. (2009). Receptive fields in primate retina are coordinated to sample visual space more uniformly. *PLoS Biol.* 7, e1000063.
- Leuba, G., and Kraftsik, R. (1994). Changes in volume, surface estimate, three-dimensional shape and total number of neurons of the human primary visual cortex from midgestation until old age. *Anat. Embryol. (Berl.)* 190, 351–366.
- Manookin, M.B., Patterson, S.S., and Linehan, C.M. (2018). Neural mechanisms mediating motion sensitivity in parasol ganglion cells of the primate retina. *Neuron* 97, 1327–1340.e4.
- Rhoades, C.E., Shah, N.P., Manookin, M.B., Brackbill, N., Kling, A., Goetz, G., Sher, A., Litke, A.M., and Chichilnisky, E.J. (2019). Unusual physiological properties of smooth monostriated ganglion cell types in primate retina. *Neuron* 103, this issue, 658–672.
- Van Essen, D.C., Anderson, C.H., and Felleman, D.J. (1992). Information processing in the primate visual system: an integrated systems perspective. *Science* 255, 419–423.
- Zadeh, L.A. (1965). Fuzzy sets. *Inf. Control* 8, 338–353.

## Loss of Nav1.2-Dependent Backpropagating Action Potentials in Dendrites Contributes to Autism and Intellectual Disability

Leonard K. Kaczmarek<sup>1,2,\*</sup>

<sup>1</sup>Department of Pharmacology, Yale University School of Medicine, New Haven, CT 06520, USA

<sup>2</sup>Department of Cellular and Molecular Physiology, Yale University School of Medicine, New Haven, CT 06520, USA

\*Correspondence: [leonard.kaczmarek@yale.edu](mailto:leonard.kaczmarek@yale.edu)

<https://doi.org/10.1016/j.neuron.2019.07.032>

Mutations in voltage-dependent sodium channels cause severe autism/intellectual disability. In this issue of *Neuron*, Spratt et al. (2019) show that lowering expression of Nav1.2 channels attenuates backpropagation of action potentials into dendrites of cortical neurons, preventing spike-timing-dependent synaptic plasticity.

There is a well-established link between the occurrence of childhood seizures and autism. More than 30% of patients

with autism have documented seizures during infancy or childhood, although in many cases the seizures decrease or

cease altogether later in development. Epileptic seizures reflect the aberrant synchronous bursting of large populations of

